Evaporation Kinetics of Tetraalkylammonium Ions from Charged Formamide Drops

Bon Ki Ku† and Juan Fernandez de la Mora*

Yale University, Mechanical Engineering Department, New Haven, Connecticut 06520-8286

Received: October 25, 2004; In Final Form: February 18, 2005

The rate of ion evaporation from the surface of electrically charged liquid drops may be inferred from observations of the minimum drop charge q present on drops of a given radius R. This critical relation $q(R)$ is measured here from the fossil solid residues left by the drops after complete solvent evaporation. We obtain mobility distributions of singly charged clusters formed by charge-reduced electrosprays of tetra-*n*-alkylammonium salts $(C_nH_{2n+1})_4N^+$ ($n = 2-10$) dissolved in formamide. These distributions exhibit modulated structures, with each wave being associated with an initial charge state of the clusters prior to charge reduction, from which critical $q(R)$ relations follow. For n from 4 to 7, the behavior is weakly dependent on the length of the alkyl chain. Above $n = 7$, there is a marked increase in solvation energy of the alkylammonium ions, but drop curvature effects contribute a compensating reduction of the energy barrier for ionization. This curvature effect increases monotonically with n and is probably associated with surface activity. Few clear modulations are seen for $n < 3$, perhaps because of the decreased role of surface activity in transferring solute into very small drops during the Coulombic breakup of larger drops. For this reason, extension of this technique to small inorganic salts is problematic.

I. Introduction

The phenomenon of electrospray (ES) ionization has been widely used (>1500 papers/year in 2001) following the discovery by Fenn and colleagues of its potential for mass spectrometric (MS) analysis of large[1] as well as small[2] ions originally in solution. Along with the practical importance of ESMS, the technique has also sparked a rebirth of interest in fundamental studies of the interaction of ions and solvents, both in the gas phase and in solution. Many related studies have taken advantage of the new experimental possibility to form gas-phase ions in a widely broadened array of masses and charge states for subsequent investigation.[3] Others have pursued the mechanisms by which these ions are evaporated from the liquid surface.[4] After an initial period of uncertainty, it has become clear that the mechanism of ion field evaporation directly from the liquid surface[5] is responsible for the production of small ions, while large and compact multiply charged clusters and globular protein ions are produced as charged residues after complete drop evaporation.[6,7]

The emerging consensus on the validity of the ion evaporation mechanism of Iribarne and Thomson[5] suggests among other things several schemes by which various important ion−solvent properties could be measured. In the past, quantities such as the Gibbs free energy of solvation ΔG_S° of an ion have been difficult to obtain, because the contributions of the cation and the anion are not readily separated in the usual thermodynamic cycles. But because ΔG_S° enters explicitly in the Iribarne and Thomson rate law (eq 1), it could be inferred from measurements of ion evaporation kinetics. Iribarne and Thomson treated ion evaporation as a single activated step governed by

$$\frac{dz}{dt} = -\frac{kT}{h} z \exp\left[\frac{\Delta}{kT}\right] \quad (1)$$

$$\Delta(z, R) = \Delta G_S^\circ - \xi(z, R) \quad (2)$$

where kT is the thermal energy, h Planck's constant, $\xi(z, R)$ the reduction in the activation energy Δ brought about by the curvature and charge on the ion-emitting liquid surface, and $z = q/e$ is the total charge (in elementary units) on a drop of radius R. Note that the use of a rate equation for a discrete variable such as z is inappropriate when z is not large. The correct treatment involves tracking the concentration of clusters with z charges and radius R, $n_z(R)$, though the net effect of carrying out the complete discrete analysis is just a slight computable shift in ΔG_S°.[8]

Rate Measurement Technique. Two different schemes have been proposed so far to measure such rates. The most direct examines the ion currents from an electrified liquid meniscus placed in a vacuum.[9] This method, however, is limited to solvents of uncommonly low volatility and will not become fully quantitative until the geometry and electric field distribution of electrified Taylor cones becomes accurately known (most likely computationally). Less direct but more amenable to precise quantification is the inference of ionization rates from charged drops through the known rate of solvent evaporation. This notion was first used by Iribarne and Thomson,[5] who argued that the time scales for solvent and ion evaporation were identical. Loscertales et al.[10] first combined a slight refinement of this idea with an inference of the electric field E on the drop surface, taken to be proportional to the droplet's measured electrical mobility. No measurement was carried out on the rapidly evolving drops themselves but on the solid residue left after complete drop evaporation, presumed to hold the same charge and to have the same radius as the drop itself at the end of its life (this presumption is generally correct, but fails for some of

* To whom correspondence should be addressed: Professor Juan Fernandez de la Mora, Yale University, Mechanical Engineering Department, 9 Hillhouse Ave, New Haven, CT 06520-8286. Phone: (1-203) 432 4347. Fax (1-203) 432 7654. E-mail: juan.delamora@yale.edu.

† Current address: National Institute for Occupational Safety and Health, 4676 Columbia Parkway, MS R-3, Cincinnati, OH 45226. E-mail: bik5@cdc.gov.

10.1021/jp040678r CCC: $30.25
Published on Web 05/13/2005

TABLE 1: Ion Evaporation Function $F(z)$[11]

$F(z)$	0.5000	0.8354	1.1111	1.3515	1.5677	1.7658	1.9498	2.1224	2.2855	2.4404
$F(z + 1/2)$	0.6778	0.9787	1.2349	1.4622	1.6688	1.8594	2.0374	2.2050	2.3639	
z	1	2	3	4	5	6	7	8	9	10

the most mobile clusters, which are metastable). This study was also limited to drops larger than a few nanometers exhibiting negligible curvature effects in (eq 1), where in the limit of high solvent dielectric constant, the barrier reduction ξ takes the simple Shottky hump form[10]

$$\xi = [e^3E/(4\pi\epsilon_o)]^{1/2} \tag{3}$$

where ϵ_o is the electrical permittivity of vacuum. In the case of very small clusters, where curvature effects are important, a refined form of the original expression of ξ given by Iribarne and Thomson (for their same physical model of a point charge interacting with a dielectric sphere of very high dielectric constant) yields[11,12]

$$\xi = e^2[F(z - 1) + \alpha]/(4\pi\epsilon_o R) \tag{4}$$

where z is the charge state of the drop prior to ion evaporation, and $F(z)$ is a known function, shown in Table 1 for z values up to 10. $F(z)$ is reported at half-integer intervals for reasons of convenience that will become clearer on reaching eq 12. Reference 11 gave $\alpha = 4/5$ for the curvature correction term in the case of small ions. Its value was subsequently corrected to $\alpha = 2/3$ by Labowsky et al.,[12] who included surface energy contributions in a fashion coherent with Born's well-known equation for ion solvation.[12] In reality, neither Born's capillary model nor its extensions accounting for curvature and charge are quantitatively reliable, while α remains an unknown quantity for the case of the relatively large ions to be studied here. We shall therefore take ΔG_S° and α as unknown parameters to be inferred from rate measurements, otherwise interpreted on the basis of the rate law (eq 1) with expression (eq 4) for the barrier reduction.

The indirect rate measurements to be made here will be based on the experimental determination of the maximum and minimum radius at which a cluster holding z charges can exist. The connection between this function and ion evaporation kinetics is straightforward once one realizes that the transition between negligible and very large values of the ion evaporation rate occurs in a small range of values of Δ very close to a certain critical value Δ^*. The reason is that $\Delta G_S^\circ/kT \approx 100$, and ξ/kT will itself need to be of the same order for ions to evaporate at observable rates. Yet, because of the exponential term, the transition from small to large rates takes place when ξ changes by only a few kT. There is, hence, essentially no ionization for $\Delta > \Delta^*$, but a single ion evaporates almost instantaneously when $\Delta < \Delta^*$. This unit charge loss then increases Δ and stops further ionization, until solvent evaporation reduces Δ again to the critical level. The threshold condition $\Delta(R, z) = \Delta^*$ then establishes a relation $R = R_{min}(z)$ marking the minimum radius that a drop of charge z may have. Consider now a drop of radius R and charge z. Initially, there is no ion evaporation, so R evolves at constant z (vertically) in a (z, R) plane, until it eventually hits the critical $R_{min}(z)$ curve. It then loses one charge at fixed R. The charge freezes again, and R continues to evolve vertically. This succession of vertical and horizontal excursions defines a staircase trajectory evolving between two critical curves $R_{min}(z) < R < R_{max}(z) = R_{min}(z + 1)$. Hence, for the particular model of charge−drop interaction embodied in eq 4, these critical conditions may be written

$$R_{min}(z + 1)/R^* = F(z) + \alpha \tag{5}$$

$$R_{max}(z) = R_{min}(z + 1) \tag{6}$$

where the characteristic radius R^* has been defined as

$$R^* = \frac{e^2}{4\pi\epsilon_o(\Delta G_S^\circ - \Delta^*)} \tag{7}$$

All of this applies to solvent drops, whose small size and very fast evolution makes the measurement of the corresponding charges and radii rather difficult, if not impossible. All we can analyze is the solid residues remaining after complete drop evaporation. The additional assumption that these residues will have the same spherical shape, volume, and charge than their almost completely evaporated precursor drop is then made to close the picture. Although this last assumption appears to be reasonable, it fails for some of the most mobile clusters, which are unstable toward loss of one charge from the dry cluster (see refs 13 and 8 and final remarks in the conclusions). Under these various hypotheses, a plot of the measured minimum cluster radius versus the function $F(z)$ should produce a straight line, whose slope and interception with the vertical axis yield R^* and $R^*\alpha$, respectively.

One must finally determine the threshold value Δ^*. This involves something akin to following the evolution of z in (eq 1), with the special care demanded by the fact that the variable z is discrete. The analysis has already been described in detail[8] and will not be repeated here. The result for small formamide drops at room temperature is

$$\Delta^*/kT = 20 \pm 1 \tag{8}$$

It only differs slightly from the much simpler Iribarne−Thomson criterion that the characteristic time for ion evaporation, $(h/kT)\exp(\Delta^*kT)$, be the same as the known characteristic time for solvent evaporation.

The experimental effort involved in obtaining minimal and maximal radii for a multitude of clusters in different charge states is considerable, as it involves the measurement of two quantities (i.e., mass and charge), and this is generally beyond the capability of mass spectrometry (except at relatively low charge states). The full exercise has already been undertaken by combining mass spectrometry and mobility in tandem[13] or by measuring mobility twice, first for the initial multiply charged ion and again after reducing its charge to unity. The complexity of this tandem analysis can be overcome through the technique of Gamero et al.,[14] consisting of determining the mobility spectrum of the full electrospray after reducing the charge state of all clusters to unity at most. The result is a series of broad modulations, the first of which is associated with singly charged particles, the second with doubly charged particles, and so on. Hence, although the charge state information is, in principle, lost upon charge reduction, it is, in fact, retained in the modulation number. Each modulation then defines a charge state z, as well as maximum and minimum mobilities. $R_{max}(z)$ and $R_{min}(z)$ then follow from known relations between mobility and size for spherical particles. We note that an experimental proof

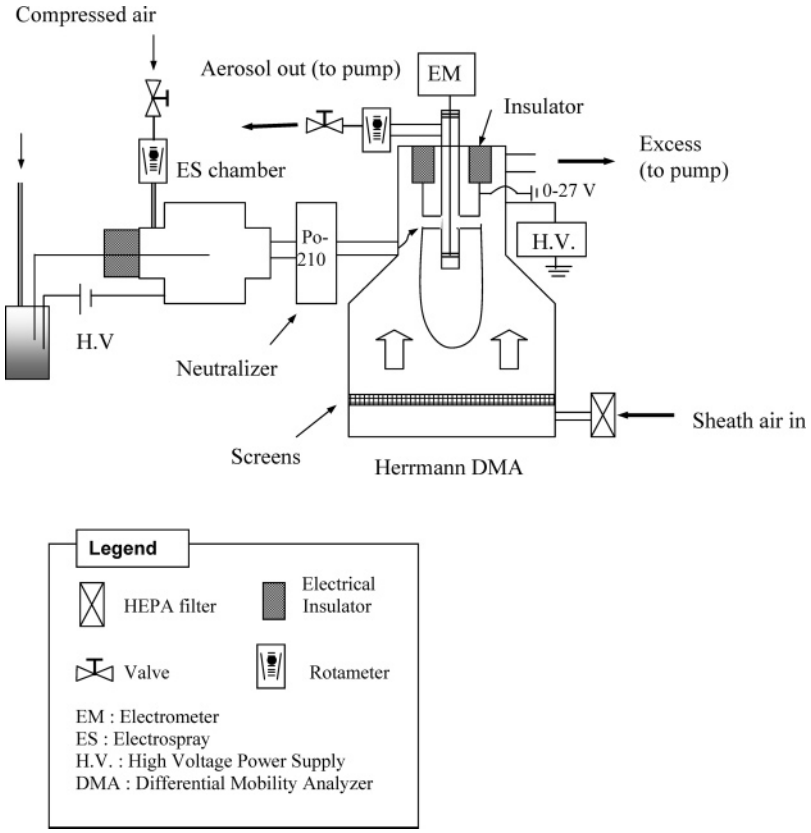

Figure 1. Experimental setup. The dry charged salt clusters (the "skeletons" of the droplets) in the ES chamber are charge-reduced to unity (single charge) by a radioactive α source (Po-210). The mobility spectrum is determined in the DMA by separating ions in space in a combined radial electric field and an axial velocity field formed between two cylindrical electrodes.

showing that each modulation corresponds to a given charge state has been given only for clusters from electrosprays of tetraheptylammonium bromide. However, as long as the charge-reduced electrosprays of other salts yield mobility distributions with similar wavy structures, the same interpretation is equally justified by analogy, as well as on the basis of the theoretical analysis available for the distribution of cluster radii of different charge states, $f(R, z)$.[8]

Plan. The goal of this article is to use the experimental technique just described to study ion evaporation from formamide solutions of various tetraalkylammonium bromides or iodides $(C_nH_{2n+1})_4N^+X^-$ ($n = 2-10$) (all alkylammonium ions used are normal, i.e., *n*-alkylammonium ions). More specifically, we will infer values of $\Delta G_S°$ and α for these various salts from observations of charge and size distributions of small clusters, formed as solid residues from evaporated electrospray drops.

II. Experimental Section

A schematic of the experimental setup is shown in Figure 1. Table 2 compiles information on the various formamide solutions used, including their composition and typical concentration. Formamide was purchased from Sigma Chemical Co. The salts were from Sigma Chemical Co. and Aldrich Chemical Co., Inc. The liquid is pushed from a 1-cm^3 polypropylene reservoir, through a silica capillary tube (20- or 40-μm i.d.), into the sharpened end of the capillary, held inside an electrospray chamber. Air is introduced in this chamber and drawn together with the dried electrospray drops through a thin plate orifice (diameter = 3.5 mm) facing the needle. On the basis of the physical properties of formamide used in refs 9−11, the initial drop diameter and evaporation time are expected to be around 140 nm and 9 ms, respectively. A typical flow rate of the air gas in this study is 4.0 L/min, and the residence time of the drops in the electrospray chamber is about 0.6 s, indicating that the formamide drops are completely dried in the electrospray chamber. The orifice communicates with a charge-reduction chamber, where a 5 mCurie ^{210}Po source (Model P-2042; NRD, Grand Island, NY) provides a bipolar ionic atmosphere which brings the charge level of the particles down to at most one elementary charge.[15] The mean direction of emission of the α particles is coaxial with the needle and the sampling orifice, but the central portion of the Po foil is covered with a thin metal surface to avoid direct irradiation of the emitting needle. This precaution is necessary, because the needle is within the range of the α particles, and the presence of negative ions in the vicinity of the positive electrospray needle tends to destabilize the spray. The electrical mobility distribution of the charge-reduced spray is then determined in a differential mobility analyzer of fairly high resolving power[16] using an electrometer as its detector (supplied commercially by Lazcano Inc.; joelaz@arrakis.es). We note that a prior study[11] used a much

TABLE 2: Various Formamide Solutions Used, Including Their Composition, Typical Concentration, Inferred ΔG, and Kinetic Parameters R^* and α (eqs 5−7) with Their Experimental Values Inferred from the Slopes and Intercepts of the Various Lines in Figure 5

solution name	composition	concn (mM)	R^* (nm)	$\Delta G_S° - \Delta^*$ (eV)	α	$\Delta G_S°$ (eV)
T-2	$(C_2H_5)_4N^+Br^-$	20	0.9346	1.539	0.188	2.045
T-3	$(C_3H_7)_4N^+I^-$	20	0.8032	1.791	0.441	2.297
T-4	$(C_4H_9)_4N^+I^-$	20	1.0053	1.431	0.320	1.937
T-5	$(C_5H_{11})_4N^+Br^-$	20	0.9889	1.455	0.374	1.961
T-6	$(C_6H_{13})_4N^+Br^-$	20	1.0133	1.420	0.370	1.926
T-7	$(C_7H_{15})_4N^+Br^-$	20	0.9746	1.476	0.443	1.982
T-8	$(C_8H_{17})_4N^+I^-$	2	0.7362	1.954	1.050	2.460
T-10	$(C_{10}H_{21})_4N^+Br^-$	2	0.7876	1.827	0.924	2.333

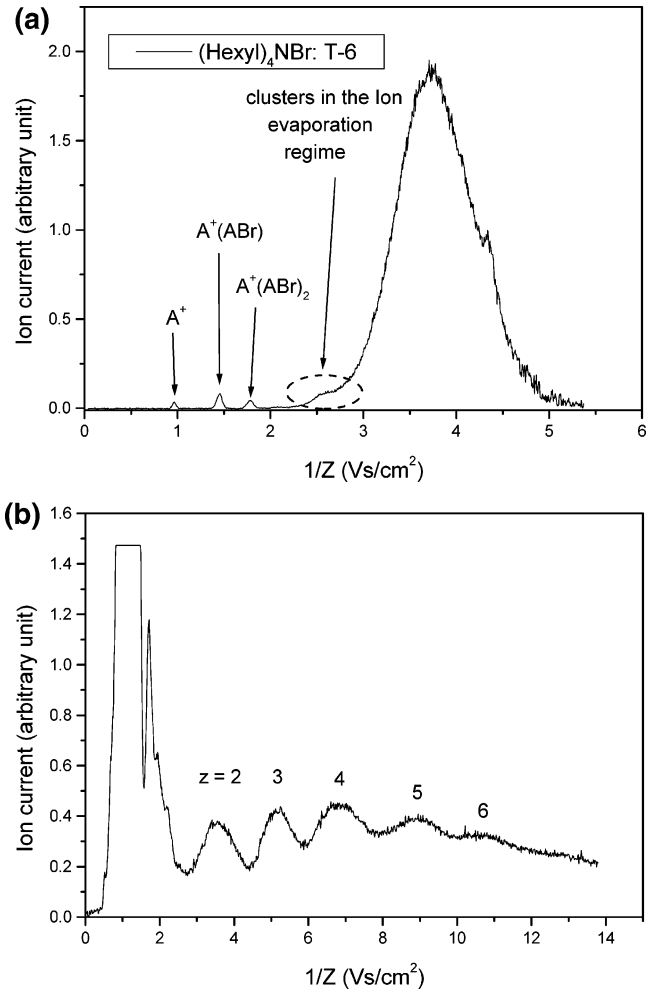

Figure 2. Inverse mobility distribution for electrosprays of tetrahexylammonium bromide (T-6) in room-temperature air, with naturally charged (nonneutralized) clusters (a) and singly charged ("neutralized") clusters (b). The isolated peaks to the left in Figure 2a are the most mobile singly charged ions. The tall peak to the left in Figure 2b is from singly charged ions produced by the electrospray and the radioactive source. Ions under the broad z^{th} modulation (counting from the left) seen in Figure 2b are associated with clusters having z charges prior to charge reduction (neutralization).[8,14] This establishes a relation between charge and cluster mobility (or radius) from which we can infer ionization kinetics.

more sensitive single ion detector (a condensation nucleus counter, CNC), but their charge-reduction chamber had a smaller ion transmission efficiency. Kaufman[17] has previously demonstrated the ability of a similar electrometer to detect small molecular clusters in another charge-reducing electrospray source of high transmission efficiency.

III. Results for Small Clusters

A typical distribution of ion abundance versus inverse mobility, $^1/_Z$, is shown in Figure 2, both with naturally charged clusters (a) and following charge-reduction (b). The drift gas is room air, and the electrosprayed salt is tetrahexylammonium bromide. The natural multiply charged spray of Figure 2a is shown at higher instrument resolution. Three different types of ions are observed in this curve. First, the spray includes relatively mobile singly charge ions (sharp isolated small peaks to the left), which are A^+, $A^+(ABr)$, and $A^+(ABr)_2$, beginning from the left, respectively, where A^+ stands for the tetrahexylammonium cation.[11,13] An initial assignment based on mobility measurement[11] has been recently corrected via mobility-MS measurement.[13] Second, the first broad shoulder to the left (marked with an ellipse and centered at $^1/_Z \approx 2.6$ V s/cm^2) corresponds to relatively small multiply charged clusters originating from drops small enough to have reached the ion evaporation regime. This point was first based on the observation that this broad peak disappears upon suppression of Coulomb explosions of droplets,[11] a point also confirmed by tandem analysis via mobility-MS.[13] Third, the second broad peak to the right (centered at $^1/_Z \approx 3.8$ V s/cm^2) comes from the solid residues of much larger drops, originally interpreted as not having reached the ion evaporation regime.[11] This point is further confirmed by the fact that these clusters are undetectable by mass spectrometry, even in instruments reaching up to $m/z = 40\,000$.[13]

Figure 2b shows a mobility spectrum of charge-reduced clusters from the same electrospray seen in Figure 2a in its natural charge state. The succession of broad modulations shown is entirely analogous to that previously described for tetraheptylammonium bromide.[14] This similarity justifies the same interpretation given in the Introduction, where each wave is associated with a charge state, increasing by one from wave to wave from left to right. In other words, before charge reduction, clusters in the second wave had two charges, those on the third wave had three, and so on.[11] As a result, we can determine the maximum and minimum mobilities (hence radii) at which each charge state arises. Readers interested in the details of how to achieve proper charge reduction should refer to prior literature.[8,15] Too little reduction leads to the survival of multiply charged peaks that distort the interpretation of the mobility information. Confirmation that the proper dose of neutralizer exposure has been achieved can be obtained by seeing the disappearance of most peaks. Those remaining are clearly singly charged, because their position remains fixed at higher neutralizing doses, while their height decreases.[8] Sharp highly mobile singly charged peaks suitable for this confirmation are not visible in the figures shown because of the low differential mobility analyzer (DMA) resolution used, but they can easily be resolved in this DMA when running under the appropriate conditions.

The complete set of charge-reduced mobility distributions obtained for the remaining solutions listed in Table 2 is shown in Figure 3. Tables 3 and 4 list as a function of the modulation number z the inverse mobilities $^1/_{Z_{mean}}$ recorded at the maximum of the modulation, as well as at the subsequent minimum ($^1/_{Z_{min}}$). Table 5 includes the cluster diameters d_p that follow for singly charged spherical particles from the mobility versus diameter relation (eqs 9−10)[18]

$$Z = 0.441 \frac{q(kT/\mu)^{1/2}}{p(d + d_p)^2} \tag{9}$$

$$\mu = \frac{mm_p}{m + m_p} \tag{10}$$

where p and m are the pressure and molecular mass of the carrier gas, $q = ze$ is the electrical charge on the cluster, and m_p is its mass. The effective mass μ is for all practical purposes identical to m. The effective diameter d of the gas molecules will be provisionally assigned the value of 0.53 nm recommended in ref 18. Data on R_{mean} (corresponding to Z_{mean} according to eqs 9−10) are plotted versus z in Figure 4 for all the substances studied.

Note in Figure 3 that the modulations are most intense for tetraheptylammonium (T-7). They become considerably weaker for T-8 and T-10 because of the low solubility of the octyl and

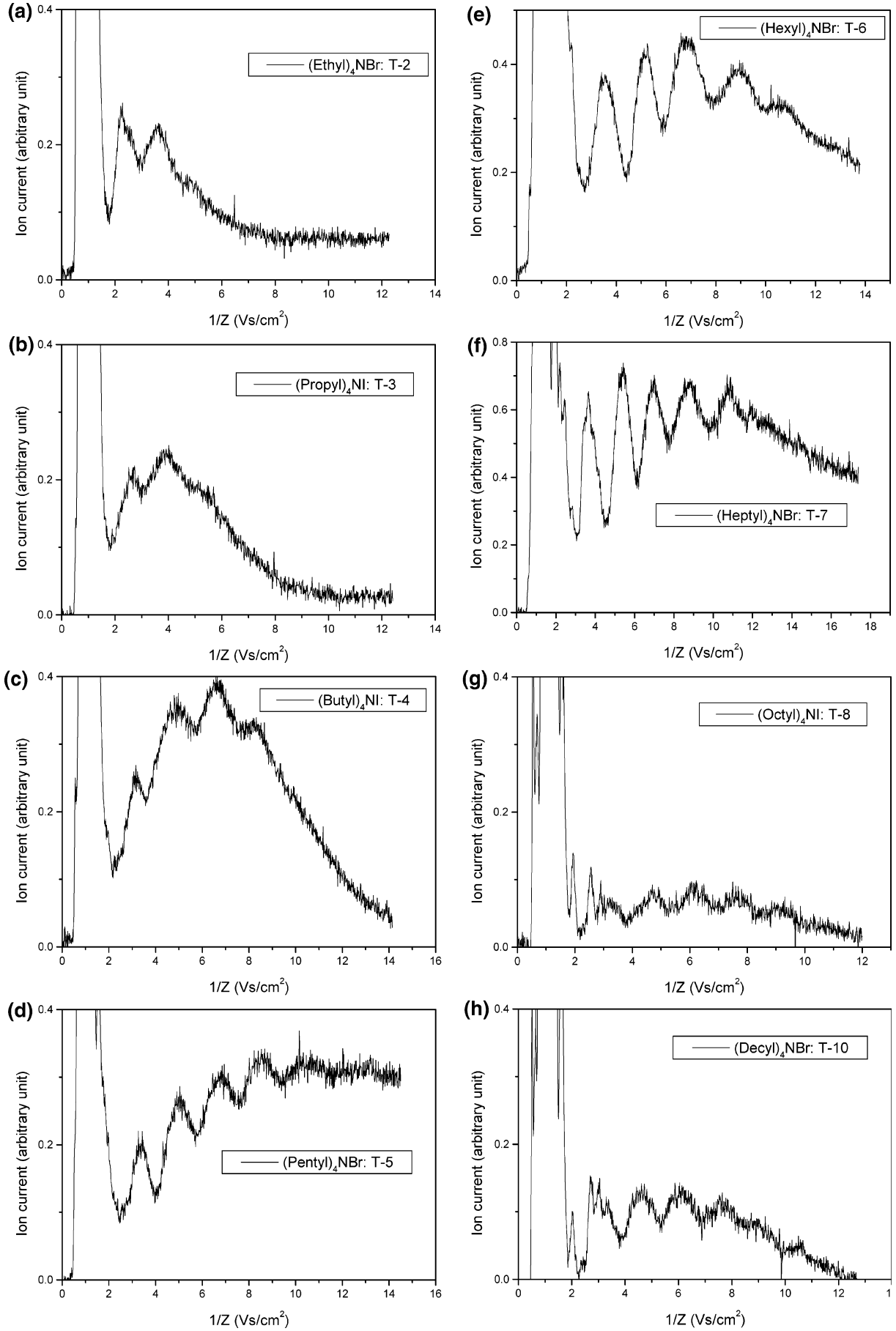

Figure 3. Inverse mobility distribution similar to those of Figure 2b, but for charge-reduced electrosprays of all other salts studied. T-2 to T-10 stand for the tetraethylammonium to the tetradecylammonium salts. Notice that fewer modulations can be seen for the lighter species.

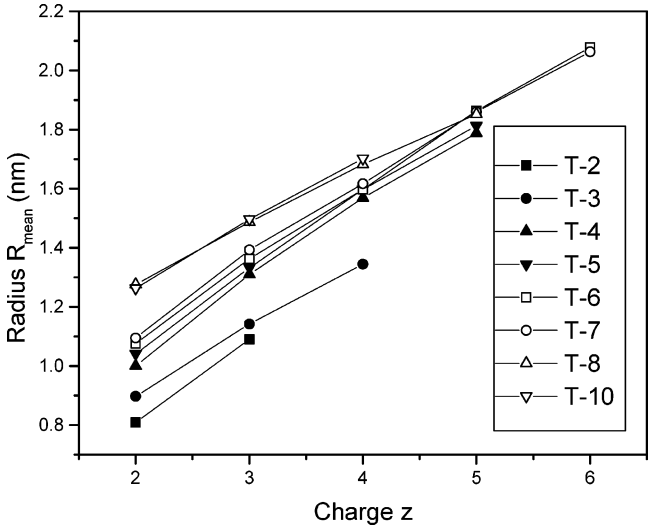

Figure 4. Curves of cluster radius $R_{mean}(z)$ at the peak of each modulation versus charge state. R_{mean} is calculated from the corresponding peak mobility and relation (9−10) between mobility and radius.

TABLE 3: Inverse Mobility $^1/_{Z_{mean}}$ (V s/cm^2) Measured at the Maximum of Each Modulation in Figures 2b and 3 as a Function of the Modulation Number (charge state) *z*

z	T-2	T-3	T-4	T-5	T-6	T-7	T-8	T-10
2	2.28	2.67	3.16	3.37	3.55	3.65	4.69	4.61
3	3.63	3.91	4.90	5.04	5.23	5.43	6.06	6.13
4		5.12	6.64	6.85	6.85	7.00	7.49	7.64
5			8.32	8.53	8.95	8.92	8.85	
6					10.84	10.71		

TABLE 4: Inverse Mobility $^1/_{Z_{min}}$ (V s/cm^2) Measured at the Right End of Each Modulation in Figures 2b and 3 as a Function of the Modulation Number (charge state) *z*

z	T-2	T-3	T-4	T-5	T-6	T-7	T-8	T-10
2	2.91	2.98	3.67	3.89	4.42	4.44	5.26	5.31
3	4.38	4.73	5.71	5.82	5.84	6.11	6.86	6.87
4		6.54	7.55	7.47	7.78	7.79	8.17	8.59
5			8.98	9.55	9.86	9.77	9.62	
6					11.84	11.72		

TABLE 5: Cluster Diameter $d_{p,mean}$ (nm) Inferred from Z_{mean} in Table 3 by Means of Eq 9 with a Gas Diameter d = 0.53 nm

z	T-2	T-3	T-4	T-5	T-6	T-7	T-8	T-10
2	1.62	1.80	2.00	2.08	2.16	2.18	2.56	2.52
3	2.18	2.28	2.62	2.66	2.72	2.78	2.98	3.00
4		2.68	3.14	3.20	3.20	3.24	3.36	3.40
5			3.58	3.62	3.72	3.72	3.70	
6					4.16	4.12		

decyl salts. As a result, the solutions sprayed are relatively dilute, have low conductivity, and spray poorly. These difficulties precluded obtaining meaningful data beyond T-10. As the length of the carbon chains decrease below seven, one sees a tendency for the modulations to become weaker, as well as a trend for the larger clusters (largest $^1/_Z$ values) to vanish. Both phenomena conspire to reduce the number of unambiguously identifiable modulations in the lighter salts to the point that only two waves can be distinguished for the tetraethylammonium sample. This tendency is stronger for tetramethylammonium (not shown), which presents only two much weaker modulations. The observation that the small ions have a lesser capacity to produce large clusters is probably associated with their decreasing surface activity. It is well-known that the succession of Coulombic explosions of the original electrospray drops produces smaller

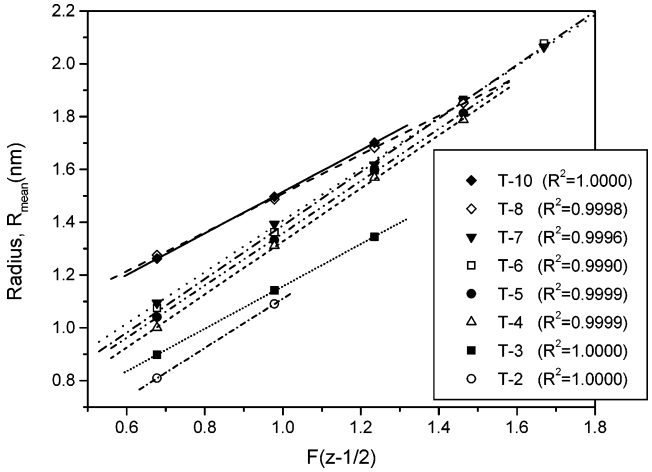

Figure 5. Curves of cluster radius $R_{mean}(z)$ versus ion evaporation function $F(z - {}^1/_2)$. On the basis of eq 11, these curves should give a straight line with slope R^* and vertical intersection αR^*. Their corresponding linear regression values yield (through eqs 7 and 8) the kinetic parameters α and ΔG_S° listed in Table 2.

drops,[1,19] and this chain of secondary atomizations eventually leads to very small drops holding only a handful of solute molecules. A number of authors have previously noted that, because daughter drops formed in Coulomb fissions carry predominantly surface material from the mother drops, they are highly enriched in surface-active solutes[20] (presumably both the cation and the anion). But because the relatively small clusters leading to the modulations seen originate from daughter drops, at a given initial salt concentration, one would expect the daughter drops to carry more solute (and hence produce larger clusters) in the case of surface-active solutes such as T-6 and T-7.

The procedure to infer ΔG and α values from the data of Figures 2 and 3 has already been discussed in the Introduction and is based on eqs 5−6, which may be written

$$R_{max}(z)/R^* = F(z) + \alpha \tag{11}$$

Hence, a plot of $R_{max}(z)$ versus the function $F(z)$ should produce a straight line, whose slope and interception with the vertical axis yield R^* and $R^*\alpha$, respectively. Alternatively, through a simple interpolation, we can rewrite eq 11 as

$$R_{mean}(z)/R^* = F(z - {}^1/_2) + \alpha \tag{12}$$

This formulation has the advantage of being based on the position of the peaks rather than the valleys of Figure 3, with corresponding values ($d_{mean} = 2R_{mean}$) tabulated in Table 5. Figure 5 shows such graphs for all the substances investigated. As found previously for tetraheptylammonium,[8] the curves are well-fit by straight lines, with fitting parameters R^*, $\xi^* = \Delta G_S^\circ - \Delta^*$ (from eq 2), and α listed in Table 2. The critical value for Δ^* required to complete the determination of ΔG_S° (reported also in Table 2) was given in eq 8 for the case of formamide.

The linear fits obtained from the data in Figure 5 are not accurate for the lighter salts, for which only two or three data points are available. However, even these few points do show a clear trend. One notices almost no variation of the slope when going from T-4 to T-7, but a slight increase in the curvature correction term α is noticeable with rising ion mass (increasing surface activity). This effect is particularly strong for T-8 and T-10. The discontinuity seen between T-7 and T-8 is somewhat surprising and has made us wonder whether the modulation

number had been accidentally displaced by one unit. However, this possibility can be rejected, by just looking at the mobility distribution data of Figure 3 for T-8 and T-10. The slope of the curves shows a clear decrease for both small and larger ions, indicating that ΔG takes a minimum at an ion molecular weight of a few hundred. Higher ΔG_S° values are to be expected for the small ions from the experimental trends previously reported for the alkali metal ions and T-1 and T-2.[21] This observed trend is not predicted by the usual Born model, where small ions cover themselves with solvent to minimize their total energy so that the nature of the ion is irrelevant. However, once the ion volume is larger than the value minimizing the free energy of the solvated ion, one should expect an increase in ΔG_S° with ionic volume, as observed. Extrapolation of the data in Figure 5 indicates that the lines for T-8 and T-10 would cross those for T-4 to T-7. A lower R at a given z (or a higher z at a given R) indicates less readiness for ion evaporation. Therefore, past the crossing point, the T-8 and T-10 ions would be less volatile than T-4 to T-7 ions. In other words, the high curvature parameter α of the large ions leads to anomalously high evaporation rates from very small drops, despite their high activation energies. This anomaly is unlikely to be observed in ordinary electrospray studies, where most of the ions originate from drops holding more than just a few charges, whereby the T-4 to T-7 ions would be expected overall to be more volatile than the T-8 and T-10 ions.

IV. Conclusions

The rate of ion evaporation from the surface of electrified liquid drops, given by the two parameters ΔG_S° and α, has been inferred from observations of charge and size distributions of small clusters formed by electrospraying formamide solutions of various tetraalkylammonium salts. The experimental technique has involved determining the maximum charge $z(R)$ retained by a cluster of radius R from mobility distributions of charge-reduced (singly charged) clusters. Our main conclusions follow.

(1) The modulations in the charge-reduced mobility spectrum are most clear and recognizable up to higher z for T-7 ($z \approx 6$), but with decreasing length of the carbon, they become fuzzier and extend to smaller z ($z = 3$ for T-2).

(2) Curves of maximum cluster radii versus $F(z)$ are linear, as expected, with slopes and intercepts defining the parameters ΔG_S° and α sought.

(3) The Gibbs free energy of solvation ΔG_S° is almost constant when going from T-4 to T-7 but takes higher values for smaller (T-2 and T-3) and larger (T-8 and T-10) ions. ΔG_S° is therefore minimal at a certain optimal ion volume. The higher activation energy found for the larger ions is expected from the Born model. The higher activation energy found for the smaller ions is not predicted by the Born model but is expected from measurements of aqueous alkali ions.[21]

(4) The constant α (accounting for an increase in ion volatility due to drop curvature) increases with the length of the alkyl group, especially for T-8 and T-10. This effect appears to be due to surface activity.

(5) We have noted the fact that the most mobile clusters are metastable and can lose one charge by ion evaporation from the solid residue. This effect has been reported previously, though only for T-7.[8] Furthermore, we have evidence for ion evaporation from dry clusters in several of the other salts studied, which form metastable doubly charged ions with electrical mobilities intermediate between those of A^+ and $(AB)A^+$. This effect tends to remove some data points in the lower right region of Figure 4 and may therefore distort the determination of the slope and intercept in Figure 5. A corresponding shift in the solvation energy as high as 0.1 eV has been recently reported,[13] and comparable errors can be expected in our new data.

Acknowledgment. This work has been supported by NSF grant CTS-9871885, AFOSR contract F-49620-01-1-1416, a gift from Rohm-Haas, and the Postdoctoral Fellowship Program of Korea Science and Engineering Foundation (KOSEF). Helpful discussions with Drs. Sven Ude and A. Nasibulin were much appreciated.

References and Notes

(1) Fenn, J. B.; Mann, M.; Meng, C. K.; Wong, S. F.; Whitehouse, C. *Science* **1989**, *246*, 64.

(2) Fenn, J. B.; Yamashita, M. *J. Phys. Chem*. **1984**, *88*, 4451; 4671.

(3) Winger, B. E.; Light-Wahl, K. J.; Ogorzalek Loo, R. R.; Udseth, H. R.; Smith, R. D. *J. Am. Soc. Mass Spectrom*. **1993**, *4*, 536. Poon, G. K.; Bisset, G. M. F.; Mistry, P. *J. Am. Soc. Mass Spectrom*. **1993**, *4*, 588. Kaufman, S. L. *Anal. Chim. Acta* **2000**, *406*, 3.

(4) Roellgen, F. W.; Bramer-Weger, E.; Buetfering, L. *J. Phys. (Paris)* **1987**, *48*, C6−253. Schmelzeisen-Redeker, G.; Buetfering, L.; Roellgen, F. W. *Int. J. Mass Spectrom. Ion Processes* **1989**, *90*, 139. Fenn, J. B. *J. Am. Soc. Mass Spectrom*. **1993**, *4*, 524. Wang, G.; Cole, R. B. *Anal. Chim. Acta* **2000**, *406*, 53.

(5) Iribarne, J. V.; Thomson, B. A. *J. Chem. Phys* **1976**, *64*, 2287. Thomson, B. A.; Iribarne, J. V. *J. Chem. Phys*. **1979**, *71*, 4451.

(6) Fernandez de la Mora, J. *Anal. Chim. Acta* **2000**, *406*, 93.

(7) Kebarle, P.; Peschke, M. *Anal. Chim. Acta* **2000**, *406*, 11.

(8) Gamero-Castano, M.; Fernandez de la Mora, J. *J. Mass Spectrom*. **2000**, *35*, 790.

(9) Gamero-Castano, M.; Fernandez de la Mora, J. *J. Chem. Phys*. **2000**, *113*, 815.

(10) Loscertales, I. G.; Fernandez de la Mora, J. *J. Chem. Phys*. **1995**, *103*, 5041.

(11) Gamero-Castano, M.; Fernandez de la Mora, J. *Anal. Chim. Acta* **2000**, *406*, 67.

(12) Labowsky, M.; Fenn, J. B.; Fernandez de la Mora, J. *Anal. Chim. Acta* **2000**, *406*, 105.

(13) Fernandez de la Mora, J.; Thomson, B. A.; Gamero-Castano, M. Tandem mobility mass spectrometry study of electrosprayed $Heptyl_4N^+Br^-$ clusters. Submitted to *J. Am. Soc. Mass Spectrom*., 2004.

(14) Gamero-Castano, M.; Fernandez de la Mora, J. *Anal. Chem*. **2000**, *72*, 1426.

(15) Kaufman, S. L.; Skogen, J. W.; Dorman, F. D.; Zarrin, F.; Lewis, L. C. *Anal. Chem*. **1996**, *68*, 1895.

(16) Eichler, T. A differential mobility analyzer for ions and nanoparticles: laminar flow at high Reynolds numbers. Senior Graduation Thesis, Fachhochschule Offenburg, Germany, 1997. The DMA used in the present study is an improvement (due to Mr. Wolfgang Herrmann) of the original Eichler DMA.

(17) Kaufman, S. L. *J. Aerosol Sci*. **1999**, *30*, S821.

(18) Fernandez de la Mora, J.; de Juan, L.; Eichler, T.; Rosell, J. *Trends Anal. Chem*. **1998**, *17*, 328.

(19) Dole, M.; Mach, L. L.; Hines, R. L.; Mobley, R. C.; Ferguson, L. P.; Alice, M. B. *J. Chem. Phys*. **1968**, *49*, 2240.

(20) Kebarle, P.; Ho, Y. In *Electrospray Ionization Mass Spectrometry*; Cole, R. B., Ed.; Wiley: New York, 1997; p 3.

(21) Tang, L.; Kebarle, P. *Anal. Chem*. **1993**, *65*, 3654 (Table 2).